Thermochimica Acta, 95 (1985) 145–153
Elsevier Science Publishers B.V., Amsterdam – Printed in The Netherlands

THERMO-OPTICAL AND THERMO-ANALYTICAL INVESTIGATIONS OF GYPSUM (CALCIUM SULFATE–WATER)

HANUS G. WIEDEMAN
Mettler Instrumente AG, CH-8606 Greifensee (Switzerland)
MICHAEL RÖSSLER
Institut für Nichtmetallische Werkstoffe, TK Claushal, D-3392 Clausthal (B.R.D.)

(Received 13 May 1985)

ABSTRACT

The experimental examples illustrate a series of possible methods for classifying gypsum and its products by using thermal analysis. In this regard, thermo-optical analysis can be used especially for observation of the rate of growth of crystals from the hydration process.

Nucleation processes in dehydration are also meaningful for the kinetics of hydration. Photographic illustrations of these processes enable the interpretation of thermoanalytical curves.

INTRODUCTION

Thermogravimetry (TG) and differential scanning calorimetry (DSC) can be regarded as the classical thermoanalytical methods for studying gypsum. Thermooptical analysis (TOA), i.e., microscopic observation of a sample on a hot stage, however, has always been less frequently used. The reasons for this are probably founded in difficulties stemming from apparatus and from

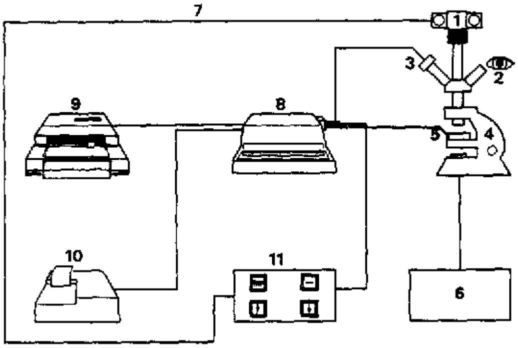

Fig. 1. Fully equipped measuring station for thermo-optical analysis. (1) Camera, (2) visual observation, (3) photometer, (4) microscope, (5) hot stage, (6) stabilized light source, (7) light cable to camera, (8) control unit FP80, (9) recorder GA17, (10) printer GA40, (11) hand controller.

the necessary experimental procedures. Today, however, the Mettler FP800 system is available for such studies. The following experiments were carried out using the Mettler FP80/84 instruments for simultaneous TOA/DSC. A diagram (Fig. 1) illustrates the configuration of the measuring instruments.

WHAT IS “GYPSUM”?

The term “gypsum”, which comes from the field of mineralogy, is used for $CaSO_4 \cdot 2\,H_2O$ (gypsum rock) found in the natural state. For the partially or completely dehydrated gypsum, the terms plaster of Paris or semihydrate are used. To avoid confusion about terms in the following text, $CaSO_4$-semihydrate will be referred to as “SH”, dihydrate as “DH” and anhydrite as “A”. If SH is added to water (“prepared”), it reacts to form DH when solidified (“set”).

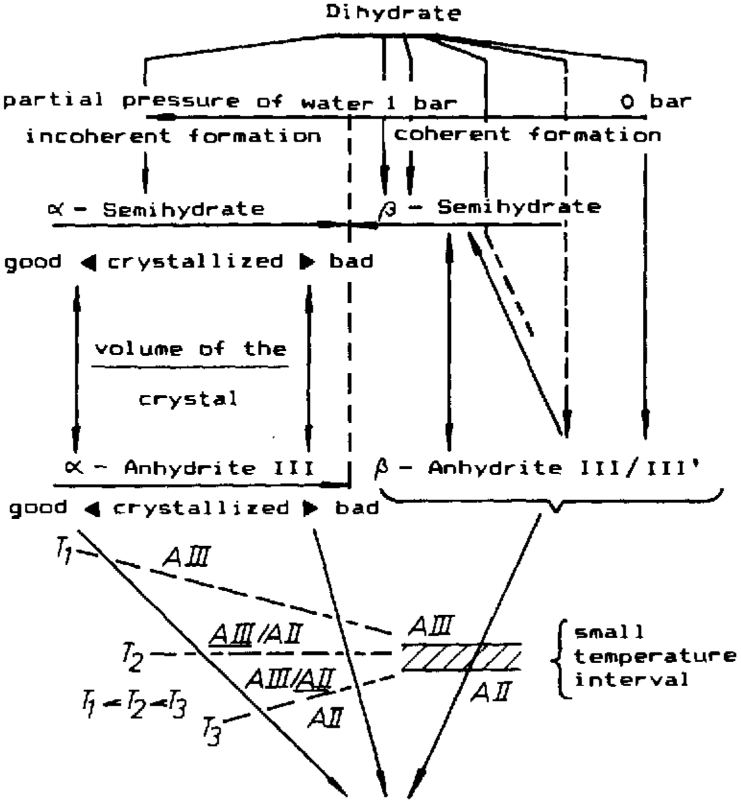

PHASES IN THE SYSTEM $CaSO_4$–H_2O

There are five phases in the $CaSO_4$–H_2O system which are listed in Table 1 along with their most important characteristics. Semihydrate and anhydrite III each have two forms with different crystallite sizes (Table 1), and thus have very different technical characteristics [1,2].

Under normal conditions (room temperature, 40–60% relative humidity), only DH (plaster) and anhydrite II are stable; SH and A III hydrate immediately in the presence of small amounts of water to the next higher hydration level; anhydrite I is stable only above 1180°C.

Exact knowledge about phase components and impurities in plaster of Paris are of the greatest engineering interest because, among other things, they influence the later material properties. Since composition can be established in the manufacturing process, it is particularly important to obtain a fast, quantitative phase analysis for controlling the process, especially of the distinction between α/β forms (Fig. 2). However, until now, this problem had not been satisfactorily solved.

HYDRATION PROCESS

Chemically, hydration proceeds according to the reaction equation $CaSO_4 \cdot 0.5\ H_2O + 1.5\ H_2O \rightarrow CaSO_4 \cdot 2H_2O$ [3–14]. There are numerous works on the hydration process that, with very few exceptions, corroborate the crystallization theory of Le Châtelier, which is 100 years old [15]. Semihydrate goes into solution until saturation is reached (8 g $CaSO_4 \cdot 0.5\ H_2O$/liter H_2O) [16]; in the formation of dihydrates, the solution is supersaturated to

TABLE 1

Phases in the $CaSO_4$–H_2O system

Name	Chemical formula	Forms	Water content (%)	Range of thermodynamic stability (°C)
Calcium-sulfate dihydrate	$CaSO_4 \cdot 2H_2O$		20.92	40
hemihydrate	$CaSO_4 \cdot 1/2H_2O$	α [a] β	6.21	metastable
anhydrite III	$CaSO_4$	α [a] β	0.02–0.05 0.6–0.9	metastable
anhydrite II	$CaSO_4$	[a]	0	40–1180
anhydrite I	$CaSO_4$		–	1180

[a] Different interpretations of forms are mentioned in the literature.

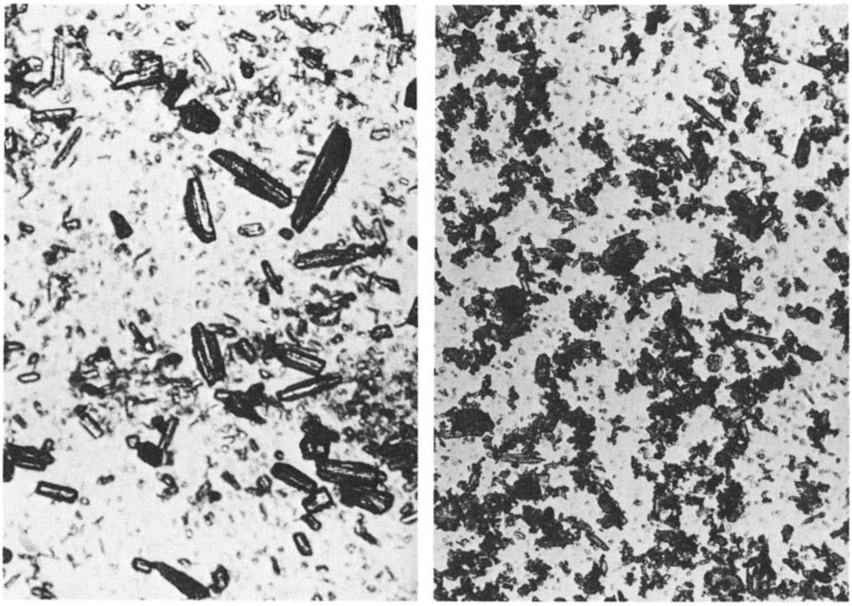

Fig. 2. α- (left) and β-Semihydrates (right) (note the particle size).

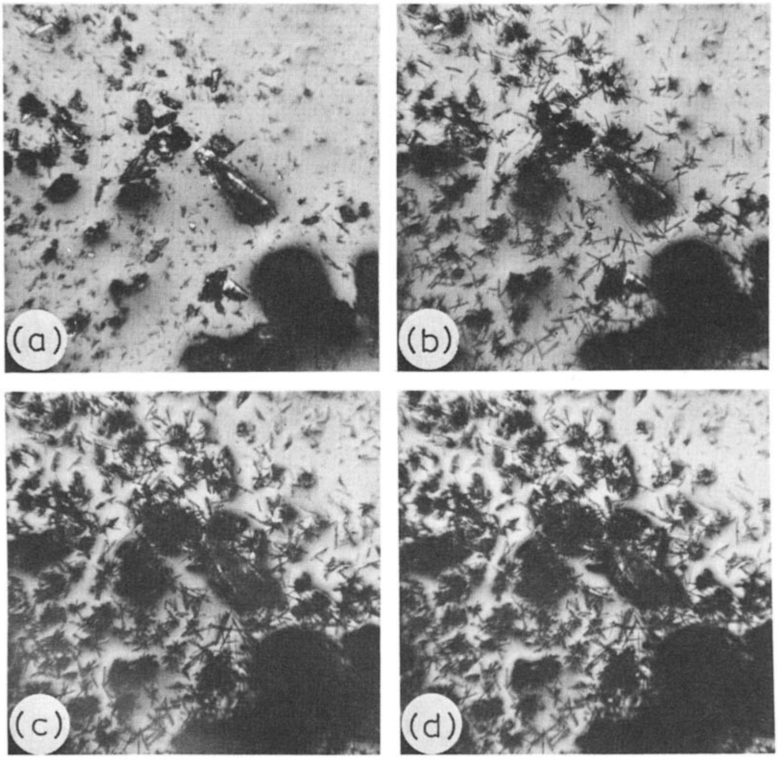

Fig. 3. Hydration process of α-semihydrate (200× magnification). (a) After 5 min, (b) after 15 min, (c) after 25 min, (d) after 45 min.

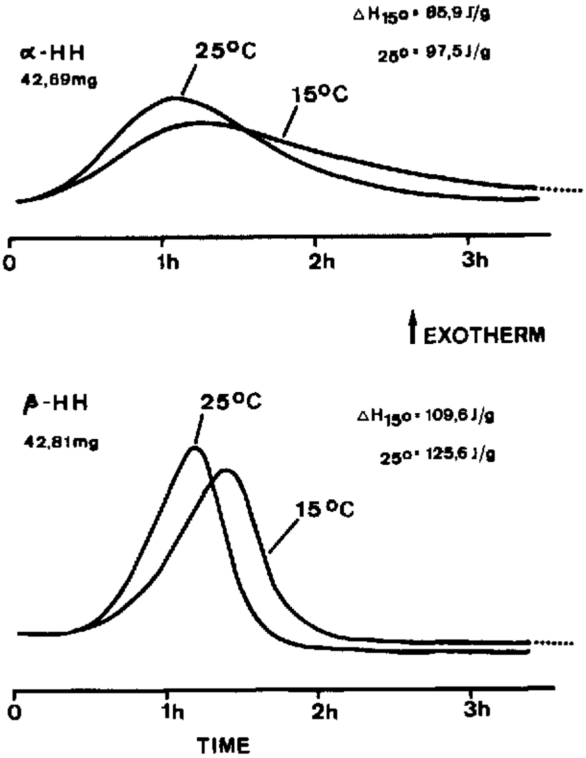

Fig. 4. Hydration rates and hydration heats, ΔH, of α- and β-semihydrates under isothermal conditions. The values of the heats of hydration are too low, i.e., the setting process is not yet complete in the illustrated curves.

DH (2 g DH/liter H_2O) [16], i.e., the dihydrate crystallizes out. For the most part, the process of hydration can be divided into four steps [17,18] (Fig. 3):

(1) Solution of the semihydrate (or anhydrous phases), dissociation into Ca^{2+} and SO_4^{2-} ions, partial formation of solvated semihydrate molecules;

(2) the primary formed hydrates are stabilized in a latent stage ("induction period") and assume a nucleus function;

(3) nucleus growth and a clear growth of dihydrate crystals;

(4) slow-down of growth as a consequence of the decreasing amount of initial anhydrous products, recrystallization.

In steps 2 to 3, further semihydrates go into solution because the concentration of SH is limited by the continuous formation of DH (similar to an autocatalytic reaction). The hydration procedure in four steps can be confirmed by using TOA (Fig. 3) and the accompanying heat of reaction can be measured using DSC. As can be seen in Fig. 4, a differentiation between pure α- and β-semihydrate forms is possible by measuring isothermal DSC curves. They also allow the determination of the heat of hydration and these indicate very good agreement with the literature values [2,3] ($\alpha = 99.7$ J g^{-1} DH; $\beta = 111.9$ J g^{-1} DH). Increasing the temperature of hydration results in the expected pronounced speed-up of the rate of reaction.

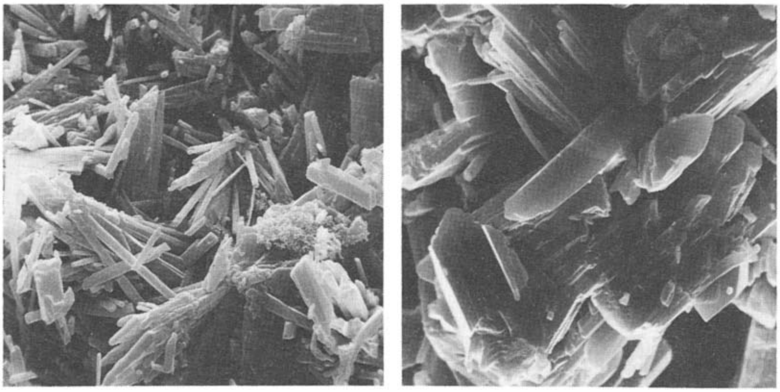

Fig. 5. Scanning electron microscope photographs of gypsum particle surfaces with and without the addition of citric acid (α; $T = 25°C$, water–gypsum ratio $= .45$; setting time: without additive, 21 min; with addition of 0.1% citric acid, 330 min).

In addition to varying the usual hydration parameters (temperature, water : plaster ratio), the rate of hydration can also be influenced by chemical additives. When this is done, in almost every case, it leads to a change in the structural arrangement and in the mechanical properties resulting from this. The effect of the various additives is very different and sometimes extraordinarily complex. The most important mechanisms for this, which are generally coupled to each other, are:

(1) change in the solubility of di- and semihydrate;
(2) change in the characteristics of nucleation;
(3) formation of protective colloids;
(4) formation of complexes;
(5) change in the transport characteristics between di- and semihydrate.

It is difficult to interpret the effect mechanisms because the influence of additives is different and sometimes even contrary, depending on the amount of additive [3]. Based on the different specific surfaces of the α- and β-semihydrates, the efficiency of the additive used depends significantly on the phase ratio of the initial mixture. Further details about this point are described in the appropriate literature [4–7].

Besides extending the setting time, the use of delayers always results in a more or less strong change in crystal formation [8]. In Fig. 5, this phenomenon is illustrated for citric acid, which is among the "ultra delayers", whereby only a few nuclei are stabilized by an extension of the induction period described above [9].

Application

Before use, e.g., for the manufacture of building materials, production of molds for the porcelain industry, etc., gypsum can be tested for quality by prior analysis. Furthermore, using this method of examination, it is possible to determine how materials from different origins react with appropriate additives.

DEHYDRATION OF SEMIHYDRATE

Dehydration of semihydrate to anhydrite III takes place in the temperature range ~ 90–180°C, whereby a difference between α- and β-semihydrates can be observed, as can be seen in Fig. 6. For the exothermal peak immediately after the endothermal dehydration peak at α, there are numerous approaches the interpretation and these range from overshooting to lamination of α-anhydrite III, as well as the immediate transformation of the α-A III to A II in the nascent state [10]. Use of this difference for quantitative analysis of the α and β contents in mixed plaster fails because the exothermal peak changes even in mixtures of pure semihydrate without correlation, or is completely missing, depending on the origin of the initial raw material. Integration of peaks for α-SH results in a reaction enthalpy of 211 J g^{-1} and of 178.4 J g^{-1} for β-SH, the latter agreeing very well with the values listed in the literature [11]. Corresponding data for α are not available in the literature. The value listed in ref. 1 (194.8 J g^{-1}) is in line with the above measurements as long as one assumes that it was a mixed plaster containing equal amounts of α and β.

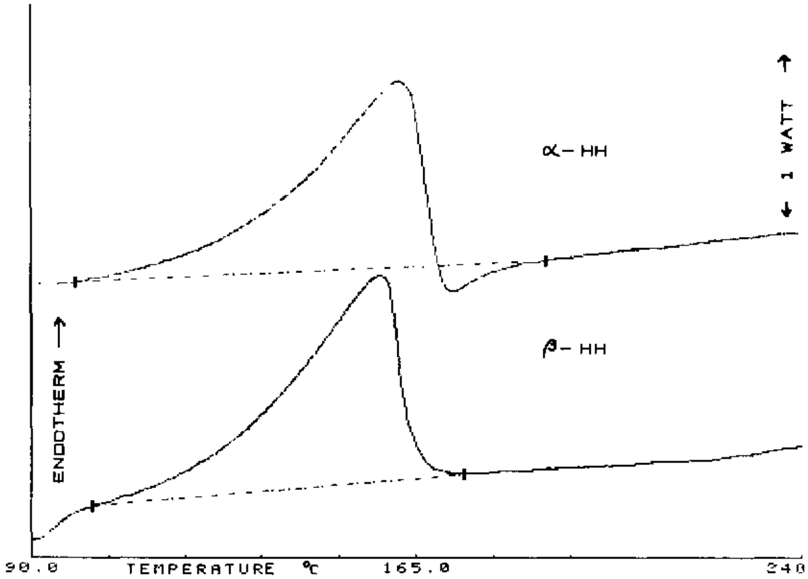

Fig. 6. DSC curves of the dehydration reactions and anhydrite transformation in the $CaSO_4$–H_2O system [14].

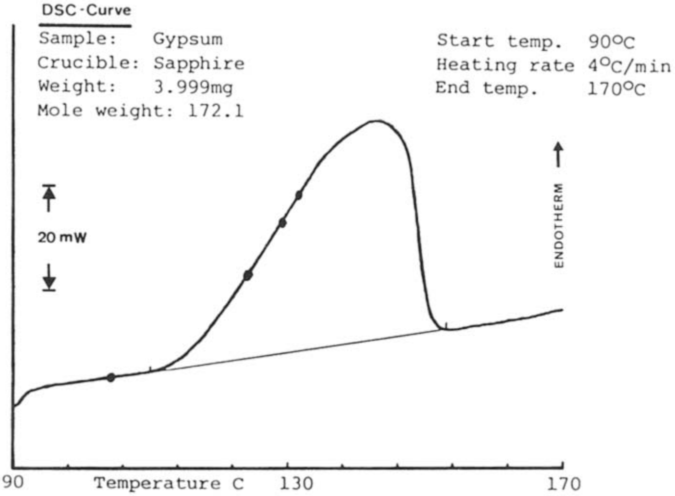

Fig. 7. DSC curve measured during dehydration. The circles on the curve correspond to the microphotographs in Fig. 8.

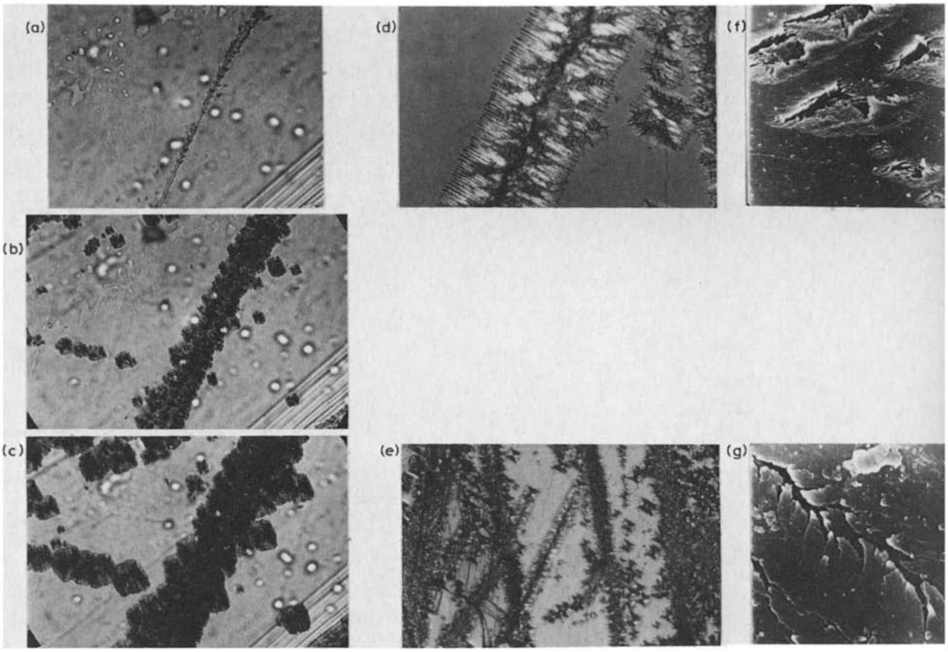

Fig. 8. Microscope photographs (50×) taken during the DSC measurement and marked by circles on the curve (see Fig. 7): (a) 104°C, (b) 124°C, (c) 129°C. Different nucleations on selenite: (d) 200×, (e) 10×. SEMs of nuclei and details of the formation of cracks: (f) 230×, (g) 2830×.

DEHYDRATION OF DIHYDRATE

Many thermoanalytical studies deal with the $CaSO_4 \cdot 2\ H_2O$ system, i.e., with dehydration of dihydrates, kinetics and the influencing parameters such as water vapor partial pressure, nucleus size and distribution, and type (or origin) of the dihydrate. Related to this are the intermediate and end products (Fig. 7), the corresponding temperatures of formation and the resulting properties [10,12,13].

The simultaneous thermo-optical photographs (Fig. 8) of DSC measurements show that nucleation in the dehydration of selenite visibly begins after the start of the separation of water. As can be expected, the first nuclei form preferably at a location where there is inhomogeneity, e.g., cracks. With the test conditions selected (vapour pressure of water ~ 30 millibar), dehydration proceeds immediately by a single-stage to γ-anhydrite III [10,12,13].

REFERENCES

1 Ullmanns Enzyklopädie der Techn. Chemie, Vol. 16, 4th edn., Verlag Chemie, Weinheim, 1976, pp. 255, 317.
2 Autorenkollektiv: Der Baustoff Gips, 1st edn., VEB-Verlag für Bauwesen, Berlin, 1978, p. 40.
3 H.E. Schwiete and A.N. Knauf, Alte und neue Erkenntnisse in der Herstellung und Anwendung der Gipse, Merziger Druckerei u. Verlags GmbH, 1967.
4 G.A. Bertoldi, Zem.-Kalk-Gips, 19 (1976) 1.
5 R.A. Kuntze, Can. J. Chem., 43 (1965) 2522.
6 M. Murat and C. Comel, Tonind.-Ztg., 95 (1971) 29.
7 M. Rössler, Dissertation, TU Clausthal, 1983.
8 E. Karmazine, M. Murat and C. Comels, Bull. Soc. Fr. Ceram., A5262/A513 (1978) 3.
9 K. Rieke, Dissertation, TU Clausthal, 1974.
10 V. Schlichenmaier, Thermochim. Acta, 11 (1975) 333.
11 P. Kurpiers, Dissertation, TU Clausthal, 1970.
12 H.G. McAdie, Can. J. Chem., 42 (1964) 792.
13 H.G. Wiedemann and G. Bayer, Z. Anal. Chem., 276 (1975) 21.
14 H.G. Wiedemann and M. Roessler, in B. Miller (Ed.), Thermal Analysis, Vol. II, Wiley-Heyden, Chichester, 1982, p. 1318.
15 H. Le Châtelier, C.R. Acad. Sci., 96 (1883) 1668.
16 D'Ans-Lax, Taschenbuch für Chemiker und Physiker, Vol. 1, Springer Verlag, Berlin, 1974, p. 261.
17 J.R. Clifton, National Bureau of Standards, Washington, DC, 1973, Tech. Note 755, pp. 1–28.
18 G. Lucas, Zem.-Kalk-Gips, 27 (1974) 233.